Constraining the nature of two Lyα emitters detected by ALMA at $z = 4.7$

R. J. Williams,[1,2]★ J. Wagg,[1,3,4] R. Maiolino,[1,2] C. Foster,[3,5] M. Aravena,[3,6]
T. Wiklind,[7] C. L. Carilli,[1,8] R. G. McMahon,[9] D. Riechers[10] and F. Walter[11]

[1]*Cavendish Laboratory, University of Cambridge, 19 J.J. Thomson Ave., Cambridge CB3 0HE, UK*
[2]*Kavli Institute for Cosmology, University of Cambridge, Madingley Road, Cambridge CB3 0HA, UK*
[3]*European Southern Observatory, Alonso de Córdova 3107, Casilla 19001, Vitacura, Santiago, Chile*
[4]*Square Kilometre Array Organisation, Lower Withington SK11 9DL, UK*
[5]*Australian Astronomical Observatory, PO Box 915, North Ryde, NSW 1670, Australia*
[6]*Núcleo de Astronomía, Facultad de Ingeniería, Universidad Diego Portales, Av. Ejército 441, Santiago, Chile*
[7]*Joint ALMA Observatory, Alonso de Cordova 3107, Vitacura, Santiago, Chile*
[8]*National Radio Astronomy Observatory, Socorro, NM 87801, USA*
[9]*Institute of Astronomy, University of Cambridge, Cambridge CB3 0HA, UK*
[10]*Department of Astronomy, Cornell University, Ithaca, NY 14853, USA*
[11]*Max-Planck Institute for Astronomy, D-69117 Heidelberg, Germany*

ABSTRACT

We report optical spectroscopy from the Very Large Telescope/FOcal Reducer and low dispersion spectroscopy of the two Lyα emitters (LAEs) companions to the quasi-stellar object–sub-millimetre galaxy system BRI1202-0725 at $z = 4.7$, which have recently been detected in the [C II]158 μm line by the Atacama Large Millimetre/Sub-millimetre Array. We detect Lyα emission from both sources and so confirm that these LAE candidates are physically associated with the BRI1202-0725 system. We also report the lack of detection of any high-ionization emission lines (N V λ1240, Si IV λ1396, C IV λ1549 and He II λ1640) and find that these systems are likely not photoionized by the quasar, leaving in situ star formation as the main powering source of these LAEs. We also find that both LAEs have Lyα emission much broader (∼1300 km s^{-1}) than the [C II] emission and broader than most LAEs. In addition, both LAEs have roughly symmetric Lyα profiles implying that both systems are within the H II sphere produced by the quasar. This is the first time that the proximity zone of a quasar is probed by exploiting nearby LAEs. We discuss the observational properties of these galaxies in the context of recent galaxy formation models.

Key words: galaxies: formation – galaxies: high-redshift – galaxies: star formation.

1 INTRODUCTION

Lyα emission is a useful probe of star formation in the young Universe and provides an effective means of discovering high-redshift galaxies. This emission can be scattered off neutral gas and dust in the interstellar medium (ISM) and intergalactic medium (IGM); therefore, observations of Lyα line emission can provide useful constraints on star formation in these galaxies. The observed Lyα emission from high-redshift galaxies is shifted into the optical band and so has the advantage that it can be observed by ground-based telescopes. Galaxies selected for their Lyα emission can be surveyed to better understand galaxy formation and evolution (e.g. Ellis 2008).

However, it is thought that the star formation traced by optical light only makes up roughly half of the total star formation occurring at high redshifts (e.g. Devlin et al. 2009). The other half is obscured by dust and molecular gas and these galaxies are often undetectable in the optical. This is not true at far-infrared (FIR) through centimetre (cm) wavelengths, which can be used to trace the dust and molecular gas which fuels early star formation. Since the development of sensitive millimetre (mm)/cm interferometers, the number of molecular lines, fine structure lines and continuum detections in high-redshift galaxies has increased dramatically (e.g. Walter et al. 2003; Wang et al. 2010; Maiolino et al. 2012; Carilli & Walter 2013). This includes the ongoing commissioning of Atacama Large Millimetre/Sub-millimetre Array (ALMA), which can detect molecular gas to an order of magnitude greater sensitivity than previous facilities. Therefore, through the combination of optical and submm observations, we can now gain a more complete picture of the history of star formation in the young Universe.

BRI1202-0725 was the first unlensed $z > 4$ system to be detected in submm continuum emission (Isaak et al. 1994; McMahon et al. 1994). Interferometric observations of molecular CO line

★ E-mail: rw480@mrao.cam.ac.uk
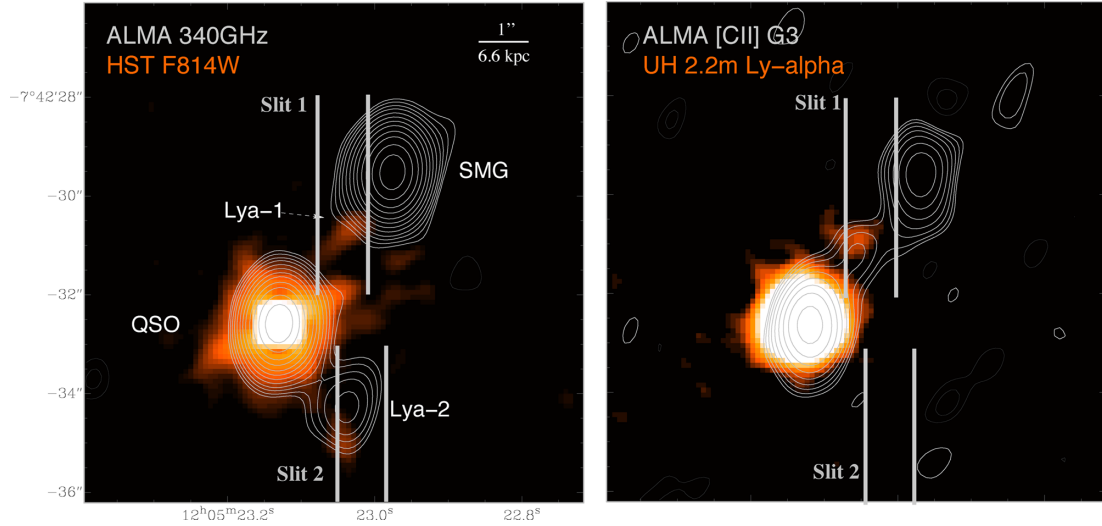
Figure 1. Image of BRI1202-0725 from Carilli et al. (2013) with the location of the FORS2 slits used to study the two Lyα sources. Left-hand panel shows the *HST* F814W image from Hu et al. (1996), while white contours show the sub-millimetre continuum detected by ALMA in Carilli et al. (2013). Right-hand panel shows the narrow band image from Hu et al. (1996) along with the integrated [C II] emission contours detected by ALMA in Carilli et al. (2013).

emission reveal a quasi-stellar object (QSO) and an optically obscured sub-millimetre galaxy (SMG) to the north-west, (Ohta et al. 1996; Omont et al. 1996), both of which are luminous in the FIR and rich in molecular and ionized gas (Omont et al. 1996; Riechers et al. 2006; Salomé et al. 2012; Wagg et al. 2012; Carilli et al. 2013; Carniani et al. 2013). In addition, narrow-band images have revealed extended Lyα emission between the QSO and SMG (Hu, McMahon & Egami 1996) and this is also seen in the continuum revealed by *HST i*-band images. This emitter is labelled Lyα-1 by Salomé et al. (2012) and is confirmed spectroscopically to be a Lyα emitter (LAE) at the same redshift as the QSO–SMG system (Omont et al. 1996; Ohyama, Taniguchi & Shioya 2004) and a few 10 kpc from the QSO. A second Lyα source is also observed at a similar distance to the south-west of the QSO (Hu et al. 1996) and is labelled Lyα-2 (Salomé et al. 2012). The redshift of this source is still ambiguous as it has not yet been spectroscopically confirmed. Recent observations of this system using ALMA detect narrow [C II] emission in the vicinity of Lyα-1, which extends from the QSO to the SMG (Carilli et al. 2013). Submm continuum emission (at 340 GHz) is likely associated with Lyα-2 (Wagg et al. 2012). The latter is also detected in [C II] by the ALMA observations (Wagg et al. 2012; Carilli et al. 2013), although at the edge of the ALMA band. Carniani et al. (2013) also claim the detection of two additional companions to the QSO and SMG. BRI1202-0725 is clearly a merging group of galaxies, likely on its way to becoming a giant elliptical in the centre of a dense cluster, therefore represents the best laboratory to date to study early massive galaxy formation.

In this paper, we use FORS2 spectroscopic optical observations to study the two LAEs in the BRI1202-0725 system, providing a larger bandwidth with extended coverage of other important lines and better sensitivity. We adopt a cosmological model with (Ω_Λ, Ω_m, h) = (0.685, 0.315, 0.673) [Ade et al. (Planck Collaboration) 2013].

2 OBSERVATIONS AND DATA REDUCTION

The FORS2 spectrograph on the VLT was used to perform multi-object spectroscopy on the system of galaxies in the field of BRI1202-0725 on the night of 2013 February 17. The 300I grating

centred at 8600 Å was used, yielding a wavelength coverage between 6000 and 11 000 Å. Slits of 4 arcsec in length and 1 arcsec in width were placed on both LAEs as in Fig. 1, as well as a selection of extended objects identified in the *R*-band pre-image. In total, six sets of observations were taken over one night, each with a 30 min exposure time.

For the data reduction process, we employ part of the FORS2 pipeline as well as self-written IDL routines to optimise the data reduction. This is because on initial inspection we find the Lyα emission to be extended and so the sky subtraction performed by the pipeline tends to remove source emission. From the raw scientific frames, we subtract the master bias and perform cosmic ray removal using an IDL script from van Dokkum (2001). This removal is based on Laplacian edge detection which relies on the sharpness of the edge of cosmic rays and therefore can be applied to single frames. The '*fors_calib*' recipe from the pipeline is used to process the calibration exposures associated with each scientific observation thus producing the normalized flat-field image, wavelength calibration coefficients and the slit positions on the CCD. These are then used as inputs for the '*fors_science*' recipe along with the science frame (post-cosmic-ray-removal) to carry out the wavelength calibration. Following this, we begin the manual sky subtraction procedure. To do this, we take the spectrum from one of the neighbouring slits with no source emission and make a one-dimensional sky spectrum which we then align with the averaged Lyα-1 spectrum over a 300 pixel sub-region. Using the best alignment parameters (so as to minimize the residuals between spectra), we re-expand the sky spectrum into two dimensions and subtract from the Lyα-1 2D spectrum. We repeat this process for Lyα-2 by performing a separate alignment for the sky with this spectrum so as to make the optimal subtraction for both cases. Finally, we perform a flux calibration by taking the calibration function obtained by the FORS2 pipeline for a standard star observation and applying it across the spectra.

We perform the reduction for each of the six observations individually to obtain six spectra, which we then align and stack together. Note that checks on the individual spectra from the reduction reveal that the seeing is similar in each observation (~0.6 arcsec); therefore, none are excluded from the stack.

3 RESULTS

In the Lyα-1 spectrum, we detect strong, extended Lyα emission with a flux of 2.53×10^{-16} erg cm^{-2} s^{-1}. This is ∼70 per cent stronger than that measured by Hu et al. (1996) with the difference possibly arising due to slit losses, although this remains unclear. The full, reduced spectrum is shown in Fig. 2. Fitting the Lyα line profile with a Gaussian gives the central wavelength of the emission at $\lambda = 6933.46$ Å which means that this source is at redshift $z = 4.703$. This is consistent with the spectroscopic redshift determined by Petitjean et al. (1996). Fig. 2 also shows that we do not detect the N v emission line, the expected location of which is shown by the arrow. In addition, we do not detect emission lines from Si IV, C IV or He II at the Lyα redshift, which we would expect to see. These non-detections are shown in Fig. 3. Note that in some cases the emission lines are located in regions partly affected by sky lines. However, we are able to compute upper limits on the fluxes for these emission lines (Table 1) and calculate the line ratios with respect to Lyα (Table 2).
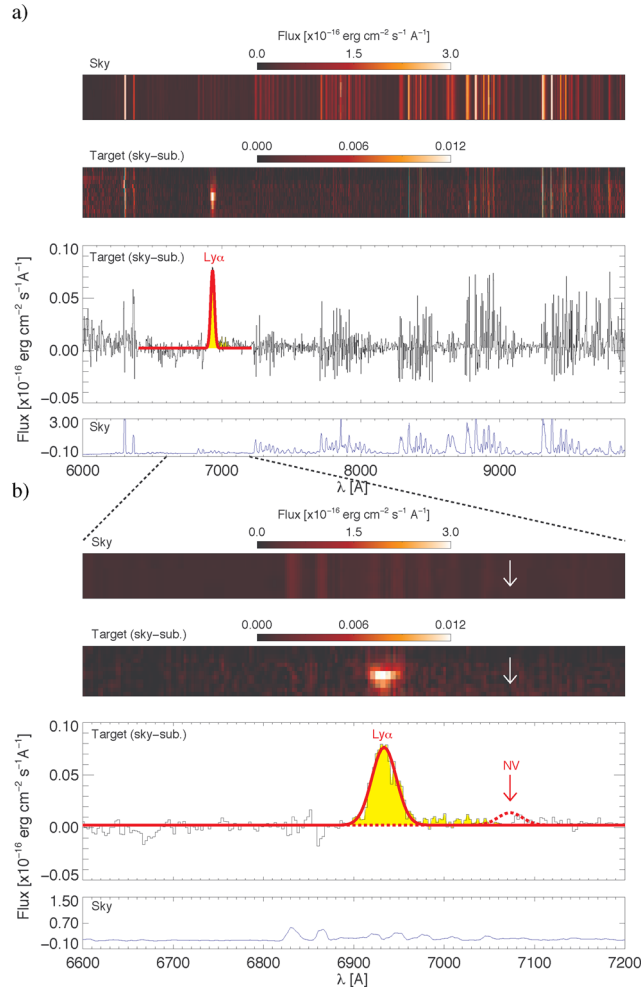
Figure 2. (a) The full extracted spectrum obtained from Lyα-1 and (b) a closer view of the Lyα emission. The panels from top to bottom show: the 2D sky spectrum, the 2D sky-subtracted galaxy spectrum, the 1D sky-subtracted galaxy spectrum and the 1D sky spectrum showing atmospheric transparency. The red line shows the Gaussian fit to the emission line. The expected location of N v is indicated by the arrow, with the dashed red line showing the expected emission profile using the average of the line ratios of QSO2s and Sy2s.
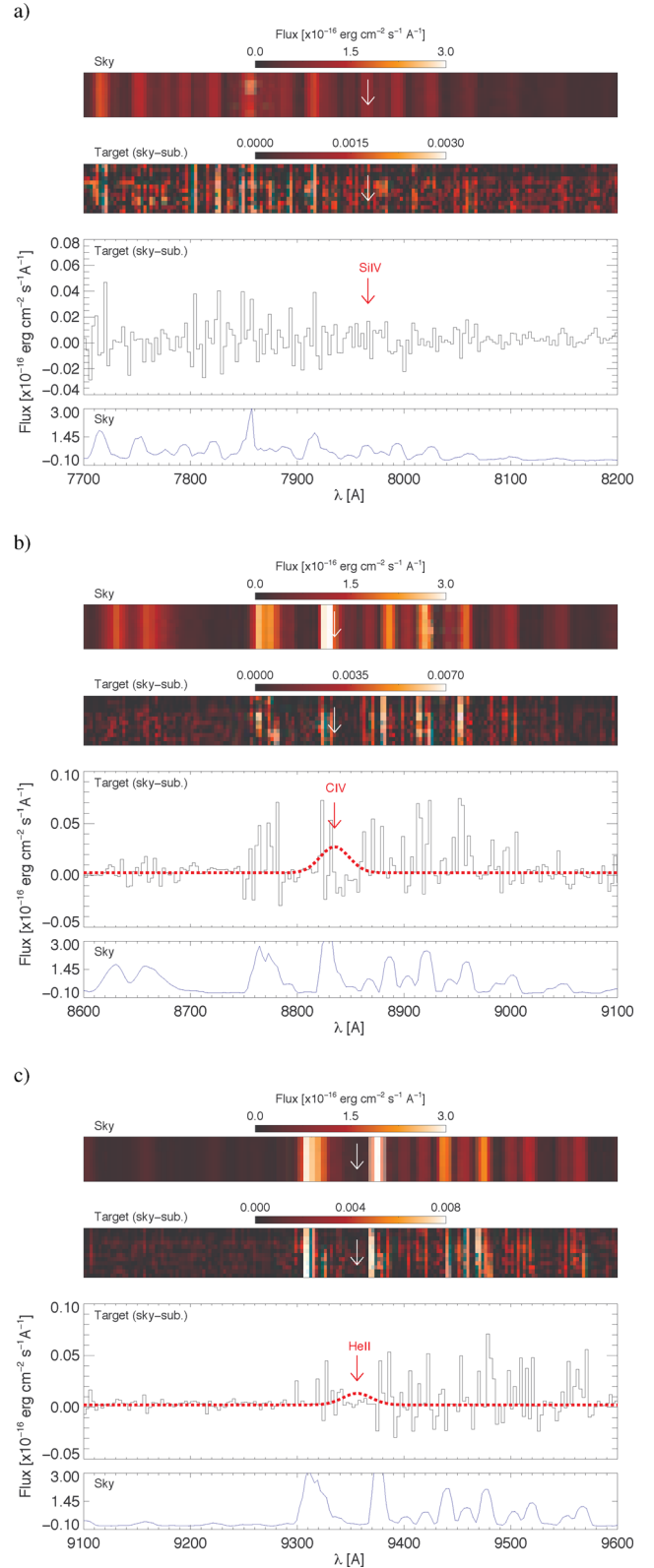
Figure 3. The extracted spectrum of Lyα-1 showing the expected location of the emission lines (a) Si IV, (b) C IV and (c) He II. The top and bottom panels show the 2D- and 1D-extracted sky spectrum, respectively, as explained in Fig. 2 caption. Again the dashed red line shows the expected emission profile using the average of the line ratios of QSO2s and Sy2s.

Table 1. Lyα line properties and upper limits on the fluxes of the other lines.

	Flux ($\times 10^{-16}$ erg cm^{-2} s^{-1})	EW (Å)	Redshift[a]	FWHM (km s^{-1})
Lyα-1				
Lyα	2.53 ± 0.08	103 ± 15	4.703	1381 ± 124
N v	<0.05	<2	–	–
Si iv	<0.04	<2	–	–
C iv	<0.08	<3	–	–
He ii	<0.05	<3	–	–
Lyα-2				
Lyα	0.33 ± 0.06	67 ± 15	4.698	1225 ± 257
N v	<0.06	<13	–	–
Si iv	<0.05	<10	–	–
C iv	<0.08	<15	–	–
He ii	<0.06	<12	–	–

[a]Error on redshift values = 0.001.

Table 2. Emission line ratio upper limits for Lyα-1 compared to the average ratios for the Nagao, Maiolino & Marconi (2006) sample of QSO2s and Sy2s.

	N v/Lyα	Si iv/Lyα	C iv/Lyα	He ii/Lyα
Lyα-1	<0.019	<0.017	<0.033	<0.018
Nagao QSO2s	0.163	–	0.337	0.149
Dispersion	0.113	–	0.167	0.074
Nagao Sy2s	0.083	–	0.284	0.159
Dispersion	0.106	–	0.212	0.072
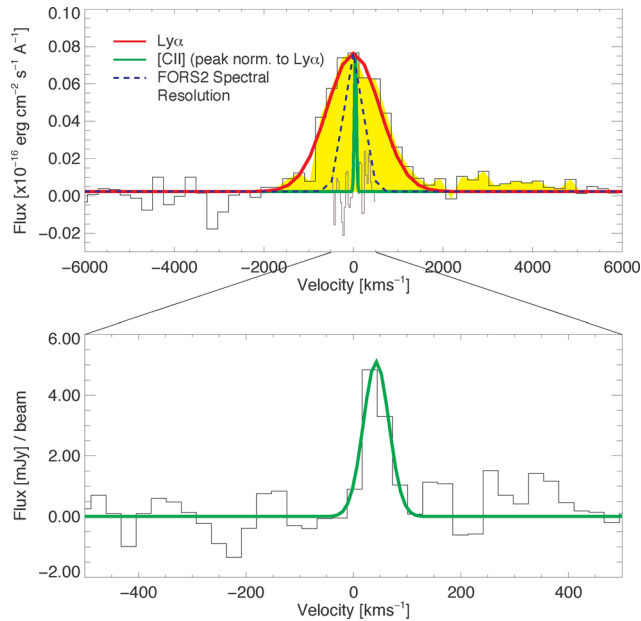
Figure 4. Comparison of the Lyα and [C ii] profiles for Lyα-1. Top: spectrum of the Lyα line (the red line shows the Gaussian fit), compared with the FORS2 instrumental resolution (blue dashed line), and with the [C ii] profile (the green line shows the associated Gaussian fit, with the peak normalized to the Lyα peak) taken from Carilli et al. (2013). Bottom: expanded view of the [C ii] spectrum.

For the Lyα-1 galaxy, we compare our Lyα profile to that of the [C ii] emission from Carilli et al. (2013), as shown in Fig. 4. We find the two profiles to be slightly shifted with respect to each other by $\Delta v = 49$ km s^{-1} and, more importantly, the Lyα line is much broader ($\sim$1400 km s^{-1}) than the [C ii] line (56 km s^{-1}).
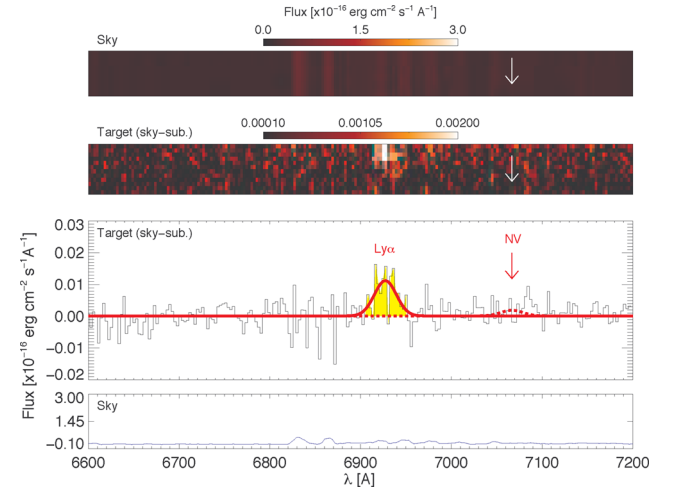
Figure 5. Lyα emission from extracted spectrum for Lyα-2. The top and bottom panels show the 2D- and 1D-extracted sky spectrum, respectively, as explained in Fig. 2 caption. The red line shows the Gaussian fit to the emission line. And again, the expected location of N v is indicated by the arrow, with the dashed red line showing the expected emission profile using the average of the line ratios of QSO2s and Sy2s.

Interestingly, we tentatively detect a high velocity tail of Lyα at the 2σ level extending to 5000 km s^{-1}, which can be seen more clearly in Fig. 4. Note that the spectral region covered by Lyα is relatively clean from strong OH sky lines.

In addition, we detect Lyα emission from the Lyα-2 galaxy, though at a much lower significance. This is shown in Fig. 5 with a flux of 0.33×10^{-16} erg cm^{-2} s^{-1}. The Gaussian fitting gives a central wavelength of $\lambda = 6927.32$ Å corresponding to a redshift $z = 4.698$. This is also slightly shifted with respect to the [C ii] emission detected from this galaxy (Carilli et al. 2013) by $\Delta v = 45$ km s^{-1} and the Lyα line is also much broader than the corresponding [C ii] line. Again, we do not detect emission lines from N v, Si iv, C iv or He ii, although in this case the upper limits on the line fluxes relative to Lyα are much less stringent than in Lyα-1. A summary of the Lyα emission properties and non-detections for both sources are shown in Table 1.

4 DISCUSSION

4.1 Lyα-1

Lyα is the only line detected in this object, all other high-ionization lines that would be expected in the case of clouds photoionized by a quasar are absent. In Table 2, we list the average ratios (and dispersion) of high-ionization emission lines observed in high-z type 2 QSOs (QSO2s) and Seyfert 2 galaxies (Sy2s) relative to their Lyα emission; these ratios are clearly much higher than the stringent upper limits obtained from our spectrum, listed in the same table. To better illustrate the expected flux of such high-ionization lines in the case of photoionization by a quasar in Figs 2 and 3, we show with a dashed profile the expected intensity of the various lines in the case of the line ratios (relative to Lyα) typical of type 2 active galactic nuclei (AGNs). Of course, if Lyα at this redshift suffers from some IGM attenuation, then the expected fluxes of the high-ionization lines should be even higher, so our expected fluxes are conservative. The lack of detection of C iv is particularly important given that this line is very strong in AGN-photoionized regions. In addition, the non-detection of He ii is also significant.

Indeed, if Lyα-1 was a system with very low metallicity, the high-ionization lines would not be detectable even in the case of AGN photoionization; however, He II should be detectable regardless of metallicity. By comparing our He II/ Lyα upper limit with the value typically observed in type 2 AGNs (see Table 2), we estimate that the fraction of Lyα produced as a consequence of ionization by the QSO must be less than 10 per cent. As a consequence, the main likely explanation for both Lyα and [C II] emission in this source is that they are powered by in situ star formation.

This source, together with Lyα-2, is one of the first $z > 3$ LAEs detected in the [C II]158 μm line. The [C II] emission (Carilli et al. 2013) together with the Sargsyan et al. (2012) conversion factor, indicate an SFR $\sim 19\,M_\odot\,yr^{-1}$ for this system, which is nicely consistent with the star formation rate (SFR) inferred from the rest-frame UV emission $SFR_{UV} \sim 13\,M_\odot\,yr^{-1}$ (Ohyama et al. 2004). We note that the size of the Lyα emission region measured in the FORS2 slit is ∼2.2 arcsec, while the 340 GHz ALMA beam is ∼1 arcsec. Since the [C II] emission is unresolved, this would imply that the [C II]-emitting region is smaller than the ionized region. This would be consistent with recent simulations of the ISM in young star-forming systems at high redshift (e.g. Vallini et al. 2013), which indeed expect strongly different distributions between ionized gas (traced by Lyα) and [C II] emission. However, it is also possible that there is a more extended [C II] emission line component below the sensitivity of current observations.

The EW(Lyα) is very high, similar to other high-z LAEs. This indicates that this is either a young system (of the order of a few million years) or is an older, very metal poor system (Schaerer 2003), though the latter is unlikely due to the detection of [C II].

The most striking feature of this system is the large width of the Lyα emission (1381 km s^{-1}), which is uncommon among any other LAEs and is accompanied by an even higher velocity tail (5000 km s^{-1}). The drastically different kinematics between Lyα and [C II] in Lyα-1 may trace an extremely inhomogeneous ISM and star formation environment in these early, young star-forming systems. This would again be in line with the strongly different distributions (hence different kinematics) between ionized gas and [C II] emission in high-z galaxies expected by recent models (Vallini et al. 2013), as a consequence of the complex ISM stratification and distribution of the UV radiation field.

However, the large velocity range traced by Lyα, at odds with the other LAE at similar redshift, remains puzzling and must be associated with the specific environment this system is residing in. More specifically, the observed high velocities may indicate that the system is subject to strong tidal shearing by either the QSO host, or the SMG, or possibly both. Within this tidally stretched system, compact clumps may be less affected by tidal forces and these may be traced by the narrow [C II]. However, the distance of these systems from the QSO and the SMG (at least a few tens of kpc, by accounting also for the redshift difference) suggests that the tidal scenario is unlikely. Ohyama et al. (2004) also suggest the possibility of superwinds originating from Lyα-1 to explain the elongated morphology; however, the width of Lyα emission is possibly too large for this scenario when compared to the theoretical velocities found for starburst-driven winds (e.g. Martin 2005; Thacker, Scannapieco & Couchman 2006).

Another interesting possibility is that this could be tracing the 'quasar positive feedback' predicted by some recent models (e.g. Ishibashi & Fabian 2012; Silk 2013; Zubovas et al. 2013). According to these models, gas ejected out of the quasar host galaxy may condense and start forming stars in the outflow. The very broad velocity profile (including the very high velocity tail) of Lyα in this star-forming system as well as the young age, ∼10 Myr (Ohyama et al. 2004) inferred from the SED fitting, would fit nicely in this scenario.

In alternative, both systems could be companions formed independently of the QSO, but their outer regions are blown away to high velocities by the QSO radiation pressure. However, in this case, one would expect that the high-velocity-ionized gas should show some signatures of photoionization by the QSO, i.e. high-ionization lines and He II in particular, which are not detected.

It is also of interest that there is a lack of asymmetry in both the two Lyα profiles, in contrast with any other LAE at such high redshift, whose Lyα blue shoulder is heavily absorbed by the intervening neutral IGM. This implies that no neutral IGM is present in the vicinity of either system, further implying that both systems are within the H II sphere produced by quasar. This is the very first time that the H II region surrounding a high-z quasar is probed with such a method. Considering the distance between the QSO and the LAEs, we can place a lower limit on the radius of the H II sphere at greater than 15 kpc.

4.2 Lyα-2

In the case of Lyα-2, we provide the first confirmation that this galaxy is an LAE at roughly the same redshift as the quasar and so part of the same group, which had still remained unclear previous to these results. The Lyα emission is much weaker than in Lyα-1, which is likely a consequence of dust obscuration. Indeed this system also shows strong FIR emission, as inferred by the ALMA continuum data (Wagg et al. 2012; Carilli et al. 2013) also implying that this system is likely more metal rich than Lyα-1. The constraints on the high-ionization lines are much looser and in principle we cannot exclude the presence of N V, Si IV, C IV or He II at a level, relative to Lyα, compatible with AGN photoionization. However, we find that the strong FIR emission ($L_{FIR} = 1.7 \times 10^{12}\,L_\odot$) cannot be explained in terms of dust heating by the QSO at the distance of Lyα-2 (even complete absorption of the quasar radiation would yield to a dust re-emitted FIR luminosity less than $2.3 \times 10^{11}\,L_\odot$) therefore is not consistent with solely dust heating from the quasar, hence, also requiring in situ star formation. Again, the width of Lyα is significantly larger than [C II], although in this case the difference is less extreme, probably because [C II] is at the edge of the ALMA band and therefore it is more difficult to measure its profile. However, the possible interpretation given for the nature of Lyα-1 (tidal shearing and result of quasar feedback), can certainly apply to this object as well. The Lyα profile of this object is also symmetric, indicating that also this object is located within the H II region produced by the quasar.

5 CONCLUSION

In summary, we have presented the results from our FORS2 spectroscopic observations of the two LAEs in the BRI1202-0725 system.

(i) We detect Lyα emission from Lyα-1 and Lyα-2, which spectroscopically confirms that these are both LAEs physically associated with the BRI1202-0725 system (Ohyama et al. 2004).

(ii) The observed Lyα emission must be produced by in situ star formation (i.e. no quasar photoionization/fluorescence), which is mostly a consequence of the lack of He II emission.

(iii) The very large velocity widths of the Lyα emission profiles (∼1100–1400 km s^{-1}, with a possible tentative tail extending to 5000 km s^{-1}) are peculiar for these two star-forming Lyα systems,

which may indicate that these are sites of induced star formation in the quasar outflow as proposed by several recent models of positive feedback.

(iv) The lack of asymmetry in the two Lyα profiles implies that no neutral IGM is present in the vicinity of either system, implying that both systems are within the H II sphere produced by the quasar. Therefore, we place a lower limit on the radius of the H II sphere at greater than 15 kpc.

ACKNOWLEDGEMENTS

REFERENCES

Ade P. A. R. et al. (Planck Collaboration), 2013, preprint (arXiv:1303.5076)
Carilli C. L., Walter F., 2013, ARA&A, 51, 105
Carilli C. L., Riechers D., Walter F., Maiolino R., Wagg J., Lentati L., McMahon R., Wolfe A., 2013, ApJ, 763, 120
Carniani S. et al., 2013, A&A, 559, A29
Devlin M. J. et al., 2009, Nature, 458, 737
Ellis R. S., 2008, Observations of the High Redshift Universe. Springer-Verlag, Berlin, p. 259
Hu E. M., McMahon R. G., Egami E., 1996, ApJ, 459, L53
Isaak K. G., McMahon R. G., Hills R. E., Withington S., 1994, MNRAS, 269, L28
Ishibashi W., Fabian A. C., 2012, MNRAS, 427, 2998
McMahon R. G., Omont A., Bergeron J., Kreysa E., Haslam C. G. T., 1994, MNRAS, 267, L9
Maiolino R. et al., 2012, MNRAS, 425, L66
Martin C. L., 2005, ApJ, 621, 227
Nagao T., Maiolino R., Marconi A., 2006, A&A, 447, 863
Ohta K., Yamada T., Nakanishi K., Kohno K., Akiyama M., Kawabe R., 1996, Nature, 382, 426
Ohyama Y., Taniguchi Y., Shioya Y., 2004, AJ, 128, 2704
Omont A., Petitjean P., Guilloteau S., McMahon R. G., Solomon P. M., Pécontal E., 1996, Nature, 382, 428
Petitjean P., Pécontal E., Valls-Gabaud D., Chariot S., 1996, Nature, 380, 411
Riechers D. A. et al., 2006, ApJ, 650, 604
Salomé P., Guélin M., Downes D., Cox P., Guilloteau S., Omont A., Gavazzi R., Neri R., 2012, A&A, 545, A57
Sargsyan L. et al., 2012, ApJ, 755, 171
Schaerer D., 2003, A&A, 397, 527
Silk J., 2013, ApJ, 772, 112
Thacker R. J., Scannapieco E., Couchman H. M. P., 2006, ApJ, 653, 86
Vallini L., Gallerani S., Ferrara A., Baek S., 2013, MNRAS, 433, 1567
van Dokkum P. G., 2001, PASP, 113, 1420
Wagg J. et al., 2012, ApJ, 752, L30
Walter F. et al., 2003, Nature, 424, 406
Wang R. et al., 2010, ApJ, 714, 699
Zubovas K., Nayakshin S., King A., Wilkinson M., 2013, MNRAS, 433, 3079

This paper has been typeset from a TEX/LATEX file prepared by the author.